


X-RAY SPECTROSCOPY OF SILICON DOPED WITH GERMANIUM ATOMS

 **Sh.B. Utamuradova¹, Sh.Kh. Daliev¹, B.R. Bokiev^{1*}, Jasur Sh. Zarifbayev²**

¹Institute of Semiconductor Physics and Microelectronics, National University of Uzbekistan, Tashkent, Uzbekistan

²Uzbek State University of Physical Education and Sport, Uzbekistan

Abstract. This paper presents X-ray diffraction results of p-Si doped with germanium and tin atoms. It was found that after heat treatment of the initial silicon sample at a temperature of 1100°C, a new energetically favorable direction of crystallites appears. It was determined that germanium and silicon atoms form bonds in high-potential regions of the silicon crystal lattice and this leads to a deterioration in its monocrystallinity, that is, to an increase in the number of polycrystalline regions. It has been discovered that tin atoms in silicon combine with oxygen atoms and form SnO₂ crystallites in the crystal lattice and this leads to an improvement in the monocrystallinity of silicon.

Keywords: Silicon, germanium, tin, single crystal, heat treatment, crystallite, crystal lattice.

***Corresponding Author:** Bakhodir Bokiyeu, Institute of Semiconductor Physics and Microelectronics, National University of Uzbekistan, Tashkent, Uzbekistan, Tel.: +998971993484
e-mail: boqiyeu@gmail.com

Received: 3 July 2024;

Accepted: 18 September 2024;

Published: 16 October 2024.

1. Introduction

It is known that expanding the energy range of sensitivity of semiconductor structures in the IR region is one of the urgent problems of optoelectronics (Ahmed *et al.*, 2024; Abdurakhmanov *et al.*, 1998; Daliev *et al.*, 2024; Saidov *et al.*, 2015; Zainabidinov *et al.*, 2022). In this regard, the study of the possibility of doping impurities into semiconductor samples based on the most studied materials, such as Ge, Si, Sn, in our opinion, is of the greatest interest (Madatov *et al.*, 2024; Utamuradova *et al.*, 2023; Dolbak & Olshanetsky, 2010; Zainabidinov *et al.*, 2019). Until now, doping impurities of semiconductor materials based on the Si<Sn> system, by analogy with Si<Ge>, was theoretically considered more promising (Dubrovsky & Tsyrlin, 2019; Ognev & Samardak, 2006; Tairov & Svetnov, 1990), but such samples were not obtained and studied. Although, in the works (Islam *et al.*, 2015; Utamuradova *et al.*, 2024), the authors reported the possibility of doping Sn and Ge impurities into single-crystalline silicon samples in the form of wafers; thorough experimental studies to study their structural and morphological properties were not carried out.

How to cite (APA):

Utamuradova, Sh.B., Daliev, Sh.Kh., Bokiyeu, B.R. & Zarifbaev, J.Sh. (2024). X-ray spectroscopy of silicon doped with germanium atoms. *Advanced Physical Research*, 6(3), 211-218
<https://doi.org/10.62476/apr63211>

In addition, the electrophysical and optoelectronic characteristics of semiconductor silicon materials depend on their constituent components, the perfection of structures, the distribution of impurity atoms and the lattice mismatch parameters of matrix and alloying elements. Therefore, the study of various structural parameters of silicon materials and the state of alloying elements is of great importance for determining their photo- and electrical properties. In our previous works (Abdurakhmanov *et al.*, 1998; Utamuradova, 2010; Zainabidinov *et al.*, 2016) studied the interaction of germanium atoms with other input silicon and arsenide gallium atoms. It has been established that the presence of Ge atoms in the Si lattice increases the efficiency of the formation of deep levels $E_C-0.42$ eV and $E_C-0.54$ eV associated with Mn in the Si lattice.

For this purpose, various structural parameters of p-Si (with a resistivity of 20 $\Omega\cdot\text{cm}$) doped with germanium and tin atoms were discovered using modern methods of structural research.

2. Experimental technique

Doping of silicon with germanium and tin atoms was carried out by diffusion from the gas phase in quartz ampoules evacuated to vacuum at a temperature of 1100°C for 2 hours. Single crystal samples of p-Si crystals ($\rho = 20$ $\Omega\cdot\text{cm}$) grown by the Czochralski method were used.

The control of the structural and phase states of the samples under study was carried out with an Empyrean Malvern X-ray diffractometer. The OriginPro2019 program was used to determine the peak maximum. X-ray diffraction measurements were carried out in the Bragg–Brentano beam geometry in the range $2\theta_B =$ from 10° to 90° continuously with a scanning speed of 0.33 degrees/min and an angular step of 0.0200 (deg).

3. Results and discussion

Figure 1 shows an X-ray diffraction pattern of the original silicon. It can be seen that the diffraction pattern contains several structural reflections of a selective nature with different intensities and two diffuse reflections at small and medium scattering angles.

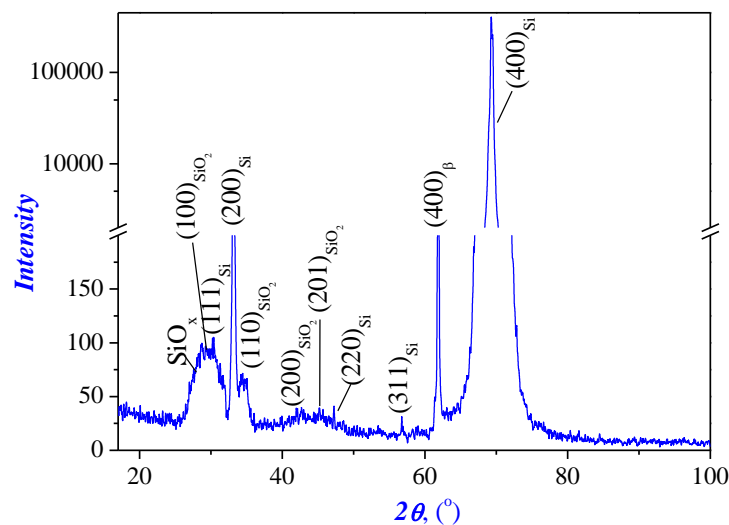


Figure 1. X-ray diffraction pattern of the original silicon samples

Analyses showed that the surface of the original silicon sample corresponds to the crystallographic plane (100). This is evidenced by the presence in the X-ray diffraction pattern of a series of selective reflections of the {H00} type, where (H = 2, 4, 5): intense lines (200) with $d/n = 0.2717$ ($2\theta = 32.97^\circ$), (400) with $d/n = 0.1362$ ($2\theta = 69.3^\circ$) and a line with weak intensity (500) with $d/n = 0.1080$ nm ($2\theta = 91.1^\circ$). The beta (β) component of the main structure line (400) is visible at a scattering angle of $2\theta = 61.75^\circ$. The high intensity ($4,5 \cdot 10^5$ imp sec⁻¹) and narrow width (FWHM= $6,1 \cdot 10^{-3}$ rad) of diffraction reflection (400) indicate the perfection of the crystal lattice of the original silicon. However, the presence in the X-ray diffraction pattern of structural lines with other indices - (111), (220) and (311) with low intensity and relatively large width compared to (400)Si, indicates the presence of polycrystalline regions in the volume of the original silicon sample. In addition, the X-ray diffraction pattern from the {H00} reflection series contains a selective reflection (200). According to the laws of extinction, these reflections should not appear on the X-ray diffraction pattern from an undistorted lattice of the diamond-like structure of silicon (Rusakov, 1977; Shulpina *et al.*, 2010; Zainabidinov *et al.*, 2021). Forbidden (200) and additional (111), (220) and (311) reflections appear in the presence of distortions in the matrix lattice caused by thermoelastic stresses arising during technological processes when obtaining samples and stresses associated with the non-uniform distribution of one of the main background impurities, namely oxygen in the silicon lattice (Babich *et al.*, 1997; Zainabidinov *et al.*, 2021; Utamuradova *et al.*, 2006).

The nonmonotonic nature of the inelastic background in the angle range from 18 to 53° is associated with residual elastic stress in the matrix lattice. At small scattering angles $2\theta \approx 27.4^\circ$, a wide (FWHM = $3,49 \cdot 10^{-1}$ rad) diffuse reflection due to structural SiO_x fragments in near-surface layers with unsaturated chemical bonds is observed in the X-ray diffraction pattern.

In addition, the diffraction pattern contains several structural reflections (100), (110), (200) and (201) related to the SiO₂ form observed at angles $2\theta \approx 26.1^\circ$ (with $d/n \approx 0.3414$ nm), $2\theta \approx 35.9^\circ$ (with $d/n \approx 0.2511$ nm), $2\theta \approx 41.5^\circ$ (with $d/n \approx 0.2174$ nm) and $2\theta \approx 44.8^\circ$ (with $d/n \approx 0.2023$ nm) X-ray diffraction patterns. This indicates the formation of SiO₂ nanocrystallites at the subcrystallite interfaces. The average size of these nanocrystallites was experimentally determined to be 38 nm. The lattice parameters are $a=b=0.4997$ nm and $c=0.5467$ nm, respectively, which, in turn, shows that the unit cell of these nano-inclusions belongs to the trigonal crystal lattice and space group P321. Thus, of all the structural lines, only reflection (400) is suitable for determining the lattice parameter of the original silicon sample, since it is the most intense and narrow (Zainabidinov *et al.*, 2022). The experimental value of the lattice parameter of the original silicon was ~ 0.5423 nm.

Figure 2 shows an X-ray diffraction pattern of silicon after heat treatment (1100°C). It can be seen that in the diffraction pattern, over the entire angular range, only 7 structural reflections with different intensities are visible, of these series there is an intense line (400) with $d/n = 0.1357$ ($2\theta = 69.15^\circ$).

Consequently, after heat treatment of the silicon sample, it is single-crystalline and its surface corresponds to the crystallographic plane (100). In the X-ray diffraction pattern, the inelastic background in the entire angular range is reduced to 42%. Also, structural reflections related to the SiO₂ form and other silicon indices (111) and (311) with weak intensity are also observed in the diffraction pattern. Only reflection (400) with strong intensity (1169 imp·sec⁻¹) and narrow width (FWHM = $1,4 \cdot 10^{-2}$ rad) is suitable for determining the lattice parameter.

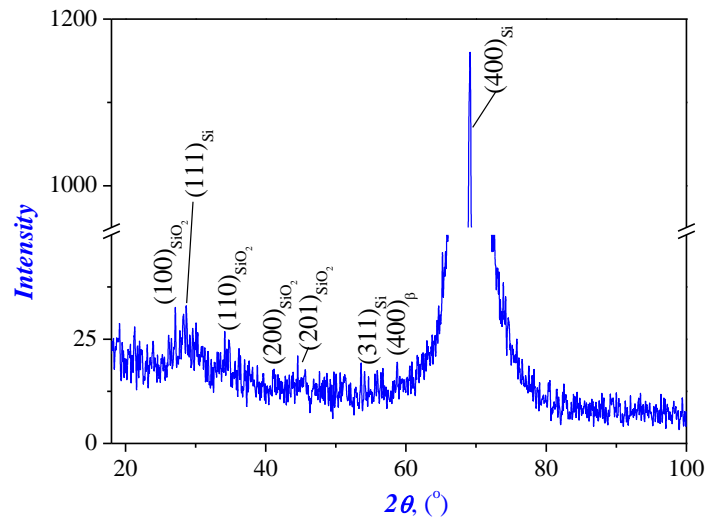


Figure 2. X-ray diffraction pattern of silicon after heat treatment (1100°C)

The experimental value of the lattice parameter of the silicon sample was ~ 0.5428 nm, which is slightly larger than the lattice parameter of the original silicon (0.5423 nm). Thus, after heat treatment of the original silicon at a temperature of 1100°C, a new energetically favorable direction of crystallites appears, due to the accumulation of elastic energy in local areas of the lattice. Consequently, the effect of annealing at a temperature of 1100°C reduces the degree of monocrystallinity of the original silicon.

Figure 3 shows an X-ray diffraction pattern of a silicon sample doped with germanium atoms at a temperature of 1100°C. It can be seen that in the diffraction pattern above the background level only structural lines (100), (110), (200) and (201) related to the SiO₂ form are observed.

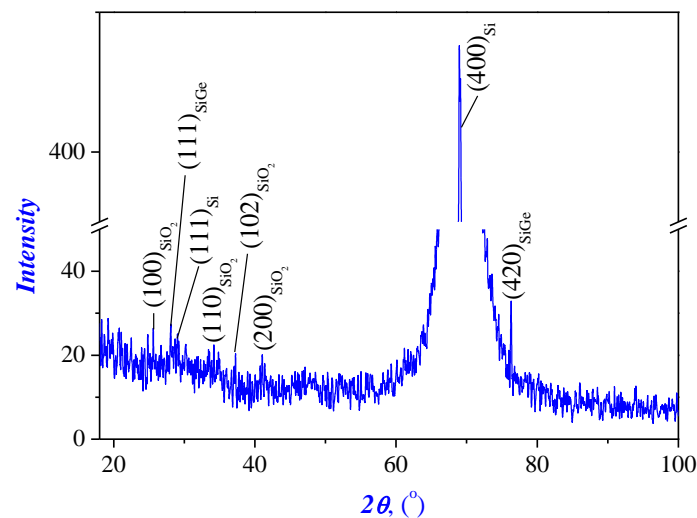


Figure 3. X-ray diffraction pattern of a silicon sample doped with germanium atoms

In the X-ray diffraction pattern of silicon doped with germanium atoms, the inelastic background is more monotonous and there are no structural reflections with other indices. Also, diffuse reflection is not observed at small scattering angles. Along with it, only a

wide and fledgling hillock, noticeable in intensity, stands out above the background level in the range of angles from 17 to 28°. A very wide maximum, more noticeable in intensity, is observed in the angle range 28-54°. The beta (β) component of the main structure line (400) is visible at a scattering angle of $2\theta = 68.9^\circ$. This main structural reflection is shifted towards small angles with respect to the main reflection observed in the X-ray diffraction pattern of silicon during heat treatment. This, in turn, indicates that when germanium atoms are introduced into the crystal lattice of silicon, its lattice parameters increase by ~ 0.0011 nm (i.e. 0.5439 nm - 0.5428 nm ≈ 0.0011 nm).

In addition, the X-ray diffraction pattern contains two lines corresponding to the crystallographic orientation (111) with $d/n = 0.3229$ nm ($2\theta = 27.6^\circ$) and (420) with $d/n = 0.1251$ nm ($2\theta = 76.11^\circ$) belonging to the covalent bond of silicon and germanium. The appearance of these lines in the X-ray diffraction pattern is associated with residual elastic stress in the silicon lattice (Zainabidinov *et al.*, 2024). This, in turn, indicates that germanium and silicon atoms form bonds in high-potential regions of the silicon crystal lattice. Therefore, their accumulation leads to the formation of various polycrystalline regions. From the values of the half-width ($\text{FWHM} = 1.7 \cdot 10^{-2}$ rad) and intensity ($442 \text{ imp} \cdot \text{sec}^{-1}$) of the main structural reflection, it is clear that they are 1000 and 2.5 times less than the intensities of the main structural lines observed in the original and annealed (1100°C) silicon samples, respectively. This, in turn, indicates that the introduction of germanium atoms into silicon at 1100°C leads to a deterioration in its monocrystallinity, that is, to an increase in the number of polycrystalline regions (Zainabidinov *et al.*, 2024).

The sample was doped with tin atoms to study and compare the effect of other dopant atoms on silicon. In Figure 4 shows an X-ray diffraction pattern of silicon doped with tin atoms.

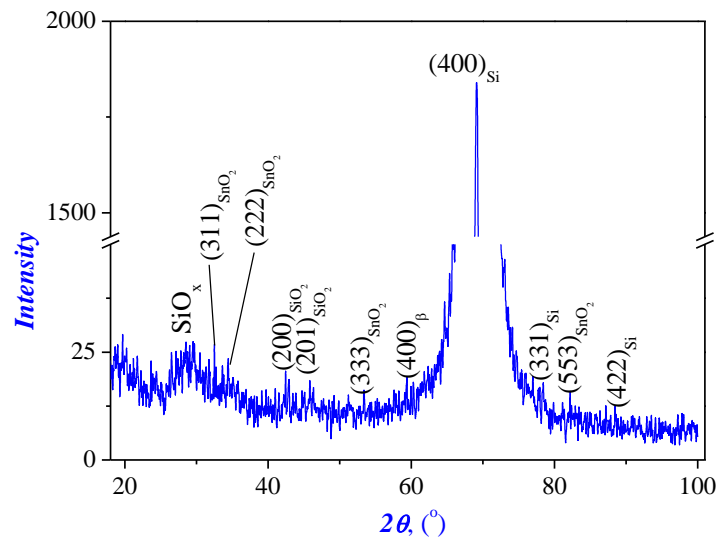


Figure 4. X-ray diffraction pattern of silicon doped with tin atoms

It can be seen that the same structural lines with strong intensity (400) with $d/n = 0.1358$ ($2\theta = 69^\circ$) are observed in the diffraction pattern. The beta (β) component of the main structure line (400) is visible at a scattering angle of $2\theta = 61.75^\circ$. Selective reflections with other indices are not present on the radiograph.

Therefore, only reflection (400) with intensity ($1843 \text{ imp} \cdot \text{sec}^{-1}$) and narrow width ($\text{FWHM} = 1.4 \cdot 10^{-2}$ rad) is suitable for determining the lattice parameter of a silicon sample

with tin impurities. The experimental value of the film lattice parameter was ~ 0.5430 nm, i.e. this value is greater than the lattice parameter (0.5428) nm of the control silicon sample. This, in turn, indicates an increase in the parameters of the crystal lattice as a result of the introduction of tin atoms into silicon. Also, the inelastic background of the X-ray diffraction pattern of silicon doped with tin atoms is non-monotonic. Diffuse reflection is clearly visible in the 2θ angle range from 18 to 48° with a maximum at $2\theta \approx 26.17^\circ$. Apparently, it is due to the inhomogeneous distribution of oxygen in the silicon lattice, since the maximum of this reflection is concentrated near the crystallographic direction [100] of the lattice of crystalline α -SiO₂. In the diffraction pattern above the background level, only structural lines (200) and (201) related to the SiO₂ form are observed. In addition, the X-ray diffraction pattern contains structural lines with other indices - (331) and (422) with low intensity and this indicates the presence of polycrystalline areas in silicon with an admixture of tin.

However, the intensity of the main structural reflection of the x-ray pattern increased by 37% compared to the control sample. This, in turn, indicates that the tin atoms in silicon combine with oxygen atoms in the crystal lattice, improving its monocrystallinity (Mansurov *et al.*, 2024). Therefore, at angles $2\theta \approx 32.8^\circ$ (with $d/n \approx 0.2728$ nm), $2\theta \approx 34.3^\circ$ (with $d/n \approx 0.2612$ nm), $2\theta \approx 52.6^\circ$ (with $d/n \approx 0.1741$ nm) and $2\theta \approx 81.8^\circ$ (with $d/n \approx 0.1178$ nm) X-ray diffraction patterns contain several structural reflections (311), (222), (333) and (555) belonging to SnO₂ crystallites. The lattice parameters of these crystallites were experimentally determined to be 0.6124 nm, which, in turn, shows that their unit cell belongs to the cubic crystal lattice and space group Fd3m.

4. Conclusion

Thus, after heat treatment of the initial silicon sample at a temperature of 1100°C , a new energetically favorable direction of crystallites appears, due to the accumulation of elastic energy in local areas of the lattice. Consequently, the effect of annealing at a temperature of 1100°C reduces the degree of monocrystallinity of the original silicon. It has been determined that germanium and silicon atoms form bonds in high-potential regions of the silicon crystal lattice and this leads to a deterioration in its monocrystallinity, that is, to an increase in the number of polycrystalline regions. It has been discovered that tin atoms in silicon combine with oxygen atoms and form SnO₂ crystallites in the crystal lattice and this leads to an improvement in the monocrystallinity of silicon.

References

- Abdurakhmanov, K.P., Daliev, Kh.S., Utamuradova, Sh.B. & Ochilova, N.Kh. (1998). On defect formation in silicon with impurities of manganese and zinc. *Applied Solar Energy*, 34(2), 73–75.
- Abdurakhmanov, K.P., Utamuradova, S.B., Daliev, K.S., Tadjy-Aglaeva, S.G. & Érgashev, R.M. (1998). Defect-formation processes in silicon doped with manganese and germanium. *Semiconductors*, 32, 606-607.
- Ahmed, B.S., Anissa, B., Radouan, N., Al Bouzieh, I., Durukan, K. & Amrane N. (2024). DFT studies on electronic, elastic, thermoelectric and optical properties of new half-heusler XRhZ (X = V, Nb and Z = Si, Ge) Semiconductors. *East European Journal of Physics*, 1, 294-307.

- Babich, V.M., Bletskan, N.I. & Wenger, E.F. (1997). *Oxygen in Silicon Single Crystals*. Interpres LTD.
- Daliev, K.S., Utamuradova, S.B., Khamdamov, J.J. & Bekmuratov, M.B. (2024). Structural properties of silicon doped rare earth elements ytterbium. *East European Journal of Physics*, 1, 375–379.
- Dolbak, A.E., Olshanetsky, B.Z. (2010). Diffusion of Sn on clean silicon surfaces. *Solid State Physics*, 52(6), 12-15.
- Dubrovsky, V.G., Tsyrlin, G.E. (2019). *Semiconductor whisker Nanocrystals: Growth, Physical Properties and Applications*. ITMO University.
- Islam, M.A., Rahman, K.S. & Haque, F. (2015). Effect of Sn doping on the properties of Nanostructured ZnO thin films deposited by co-sputtering technique. *Journal of Nanoscience and Nanotechnology*, 15(11), 9184-9191.
- Jafarov, M.A., Nasirov, E.F., Kazimzade, A.H., & Jahangirova, S.A. (2021). Synthesis and characterization of nanoscale material ZnS in porous silicon by chemical method. *Chalcogenide Lett.*, 18(12), 791-795.
- Madatov, R.S., Alekperov, A.S., Nurmammadova, F.N., Ismayilova, N.A. & Jabarov, S.H. (2024). Preparation of n-Si-P-GaSe heterojunctions based on an amorphous GaSe layer without impurities and study of their electrical properties. *East European Journal of Physics*, 1, 322-326.
- Mansurov, K.J., Boboev, A.Y. & Urinboev, J.A. (2024). X-ray structural and photoelectric properties of SnO₂, ZnO, and Zn₂SnO₄ metal oxide films. *East European Journal of Physics*, 2, 336–340.
- Mammadov, H.M., Jafarov, M.A., Nasirov, E.F., & Piriyeva, D. (2021). Photoelectrical properties of p-Si/Cd_{1-x}Zn_xS (Se)(Te) y heterojunctions. *Chalcogenide Letters*, 18(1), 31-38.
- Ognev, A.V., Samardak, A.S. (2006). Spintronics: Physical principles, devices, prospects. *Bulletin of the Far Eastern Branch of the Russian Academy of Sciences*, 4, 70-80.
- Rusakov, A.A. (1977). *X-ray of Metals*. Moscow: Atomprint. (In Russian).
- Saidov, A.S., Zainabidinov, S.Z., Kalanov, M.U., Boboev, A.Y. & Kutlimurotov, B.R. (2015). Peculiarities of photosensitivity of n(GaAs)-p(GaAs)_{1-x-y}(ZnSe)_x(Ge₂)_y structures with quantum dots. *Applied Solar Energy*, 51(3), 206–208.
- Shulpina, I.L., Kyutt, R.N., Ratnikov, V.V., Prokhorov, I.A., Bezbakh, I.Zh. & Shcheglov, M.P. (2010). Methods of X-ray diffraction diagnostics of heavily doped semiconductor single crystals. *Journal of Technical Physics*, 80(4), 105-114.
- Tairov, Y.M., Tsvetnov, V.F. (1990). *Technology of Semiconductor and Dielectric Materials*, Higher School.
- Utamuradova, Sh.B, Matchonov, K., Khamdamov, J.J. & Utemuratova, K. (2023). X-ray diffraction study of the phase state of silicon single crystals doped with manganese. *New Materials, Compounds and Applications*, 7(2), 93–99.
- Utamuradova, Sh.B. (2010). IR spectroscopy of silicon doped with germanium during growth. *Reports of the Academy of Sciences of the Republic of Uzbekistan*, 4, 26-28.
- Utamuradova, Sh.B., Bokiye, B.R. & Pulatova, D.S. (2024). Structural features of silicon with tin impurity. *East European Journal of Physics*, 2, 353-357.
- Utamuradova, Sh.B., Daliev, Kh.S., Kalandarov, E.K. & Daliev, Sh.Kh. (2006). Features of the behavior of lanthanum and hafnium atoms in silicon. *Technical Physics Letters*, 32(6), 469-470.
- Zainabidinov, S.Z., Boboev, A.Y., Makhmudov, Kh.A. & Abduazimov, V.A. (2021). Photoelectric Properties of n-ZnO/p-Si Heterostructures. *Applied Solar Energy*, 57(6), 475-479.
- Zainabidinov, S.Z., Saidov, A.S., Boboev, A.Y. & Usmonov, J.N. (2021). Features of the Properties of the surface of (GaAs)_{1-x-y}(Ge₂)_x(ZnSe)_y semiconductor solid solution with ZnSe quantum dots. *Journal of Surface Investigation: X-ray, Synchrotron and Neutron Techniques*, 15(1), 94–99.

- Zainabidinov, S.Z., Saidov, A.S., Kalanov, M.U. & Boboev, A.Y. (2019). Synthesis, structure and electro-physical properties n-GaAs-p-(GaAs)_{1-x-y}(Ge₂)_x(ZnSe)_y heterostructures. *Applied Solar Energy*, 55(5), 291-308.
- Zainabidinov, S.Z., Utamuradova, Sh.B. & Boboev, A.Y. (2022). Structural peculiarities of the (ZnSe)_{1-x-y}(Ge₂)_x(GaAs_{1-δ}Bi_δ)_y solid solution with various nanoinclusions. *Journal of Surface Investigation: X-ray, Synchrotron and Neutron Techniques*, 16(6), 1130–1134.
- Zainabidinov, S.S., Boboev, A.Y. & Yunusaliyev, N.Y. (2024) Effect of γ -irradiation on structure and electrophysical properties of S-doped ZnO films. *East European Journal of Physics*, 2, 321–326.
- Zaynabidinov, S.Z., Saidov, A.S., Leiderman, A.Yu., Kalanov, M.U., Usmonov, Sh.N., Rustamova, V.M. & Boboev, A.Y. (2016). Growth, structure and properties of GaAs-Based (GaAs)_{1-x-y}(Ge₂)_x(ZnSe)_y epitaxial films. *Semiconductors*, 50(1), 59-65.
- Zaynabidinov, S.Z., Saidov, A.S., Boboev, A.Y. & Abdurahimov, D.P. (2022) Structure, morphology and photoelectric properties of n-GaAs-p-(GaAs)_{1-x}(Ge₂)_x heterostructure. *Herald of the Bauman Moscow State Technical University, Series Natural Sciences*, 72-87.
- Zaynabidinov, S.Z., Yuldashev, S.U., Boboev, A.Y. & Yunusaliyev, N.Y. (2024) X-ray diffraction and electron microscopic studies of the ZnO<S> metal oxide films obtained by the ultrasonic spray pyrolysis method. *Herald of the Bauman Moscow State Technical University, Series Natural Sciences*, 112(1), 78-92.